



CARITAS UNIVERSITY AMORJI-NIKE, EMENE, ENUGU STATE

Caritas Journal of Engineering Technology

CJET, Volume 2, Issue 1 (2023)

Article History: Received: August 21st 2022 Revised: October 23rd 2022 Accepted: December, 2nd 2022

Assessment of selected Properties of Rice Husk -Derived Graphene - Modified with Green Synthesized Silver Nanoparticles / Polyester Nanocomposite

Ezeh, Ernest M.

Department of Chemical Engineering,
Caritas University Amorji Nike, Enugu, Nigeria
Correspondence: ezehernest@caritasuni.edu.ng

Abstract

Rice husk-derived graphene, doped with silver nanoparticles and polyester nanocomposites, was developed to explore its potential application as a conductive material for engineering applications. This research aims to develop conductive rice-husk graphene nanoparticles (Gr.NPs) mixed with orange juice-modified silver nanoparticles (Ag.NPs). This modified graphene was used to fabricate nanocomposites based on a polyester matrix. Nanocomposites were developed, and their electrical, thermal, microstructural, and mechanical properties were analyzed using standard analytical instruments. Electrical conductivity (2.08×10^{-8} S/m), dielectric constant (5.95), and thermal conductivity ($1.45 \text{ Wm}^{-1}\text{K}^{-1}$) were obtained due to the high electron mobility of AgNPs and GrNPs, which increased the electrical conductivity of the polyester. An improved tensile strength of 92.35% was achieved for the developed nanocomposite. The AgNPs ensured good dispersion of the GrNPs in the polymer matrix. Consequently, rice husk finds application in the development of conductive polyester-graphene nanocomposites for a wide range of Engineering applications.

Keywords: Characterization, graphene, nanocomposites, rice husk.

1.0 Introduction

Over the past few decades, polymeric materials, have largely replaced many traditional materials in a variety of applications from kitchen utensils to mechanical workings. This is possible thanks to the advantage of polymers over traditional materials [1,2]. Cost saving, easy processing, easy processing, low density, damping of sound and vibration, corrosion resistance, mechanical strength and other advantages are some of them [3,4]. However, they have several disadvantages, including poor thermal stability; can oxidisation at high temperatures. They often have limited conductivity and resistance when saturated.[5] Polymer nanocomposites have therefore been the subject of intensive research over the past 30 years. Conductive composites are particularly important because they outperform traditional metal and rare earth devices in terms of antistatic coatings and flexible electronics.[6] Various compounds have been added to plastics to create conductive composites. Metal fibres and glass fibre particles coated with aluminium, steel, iron, copper and nickel were used [7]. Several carbonaceous materials including carbon black, carbon fibre,

graphite and carbon nanotubes (CNTs) have been used to improve electrical conductivity [8]. However, graphene outperforms these carbonaceous materials in several areas, including excellent charge-carrier mobility at room temperature ($250,000 \text{ cm}^2\text{V}^{-1}\text{s}^{-1}$), mechanical strength (Young's modulus 1TPa), electrical conductivity ($6,000 \text{ Scm}^{-1}$), thermal conductivity ($5000 \text{ Wm}^{-1}\text{K}^{-1}$) and large surface area ($2600 \text{ m}^2\text{g}^{-1}$) [9]. When the concentration of these charges reaches a certain point, the charged particles collide, creating a continuous channel through which the electrons travel. This concentration level of charges is called the percolation threshold [10,11]. The shape of the conductive filler strongly influences the percolation threshold. For example, for three standard fillers with an approximately spherical shape, filler contents of 10–20% by weight are required [12,13].]. When using carbon nanotubes as conductive fillers, a carbon black content of 8 to 40% by weight is required. Filler content 1-20% by weight. it is necessary for marketing. dependent on the content required for effective use [14,15]

With electricity powering a wide variety of devices, sensors, and devices, designing and manufacturing a material that successfully conducts electricity has become an important area of research in modern life [16,17]. Thanks to its excellent electrical conductivity and mechanical strength. However, the development of an electrically conductive polymer composite was highly demanded due to its many advantages including high chemical stability and corrosion resistance, lightweight, better processability and low production cost [18,19]. Conductive fillers such as graphite, carbon fibres, carbon black, metal fibres, graphene, metal powder, carbon nanotubes (CNT), etc. are successfully used in the production of conductive polymers [20, 21]. In all the conductive fillers listed, graphene has proven to be an interesting application to produce a conductive polymer [22]. Despite the unique properties of graphene-graphite nanosheets (Gr.NP), the application of their polymer nanocomposites are sometimes unsatisfactory. Nanofiller agglomeration is one of many other reasons for this failure but is still poorly studied [23,24]. The project aims to study and improve some engineering properties of polyester nanocomposites by enriching them with graphene obtained from rice husks coated with orange juice-modified silver nanoparticles. Minimizing agglomeration and improving the electrical, thermal and mechanical properties of the developed nanocomposites.

2.0 Methods

2.1 Materials

A thermosetting unsaturated polyester resin was used in the tests. Vaseline was used as a mould-release agent to prevent the polyester from sticking to the mould when demolding. Tony Chemical Enterprise of Enugu, Nigeria supplied other ingredients such as cobalt naphtholates and methyl ethyl ketone (MEK) peroxide, and rice hulls were collected from rice mills in Abakaliki, Ebonyi, Nigeria. Rice husks were thoroughly cleaned and rinsed with tap water to remove dirt, then dried in the sun for a month before being ground into powder ($75 \mu\text{m}$) (Figure 1). Cashew leaf extract was used to prepare Ag.NPs. The fresh cashew leaves used in this work were sourced from the surrounding area of Caritas University in Enugu State, Nigeria.



Figure 1: Photograph of waste rice husk for the synthesis of Graphene

2.2. Production of Graphene from Rice Husk

Rice husk (RH), a high-volume and renewable waste in Nigeria, was used as the starting material in this study. Potassium hydroxide (KOH), a chemical reagent, was used to create porosity. The process to produce graphene oxide from rice hulls has been slightly modified [25, 26]. Graphene is synthesized from charred rice husk (CRH) in four steps: pre-carbonization, drying, activation, and exfoliation. RH was washed in distilled water many times to get rid of impurities, then dried at 110°C for 1 hour. Relative humidity was charred in a rotating reactor in an inert medium at a temperature of 250-300°C with an argon flow of 5 cm³/min and a char time of 45 minutes [27-29]. The CRH samples were immersed in 3L of 1M sodium hydroxide (NaOH) solution and heated at 110°C for 3 hours to remove SiO₂ and then allowed to settle. To eliminate froths, RH was cleaned quite a few times with distilled water and then dried at 110°C for one hour. RH was charred in an inert rotary reactor at 250-300°C with an argon flow rate of 5 cc/min and a char time of 45 minutes [30,31]. The charred samples (CRH) were immersed in 3L of a 1M NaOH solution, heated at 110° for 3 hours to remove SiO₂ and then allowed to decant. The argon was fed at a rate of 5 standard cubic centimetres per minute (SCCM) to prevent oxidation (standard cubic centimetres per minute). After activation, the samples were washed several times with distilled water until pH 7 and the filtered samples were dried at 100 °C for 24 hours [32]. The CRH was exfoliated in a hydrogen peroxide solution (H₂O₂.37%) for 48 hours to free the amorphous carbon layers from the samples. After the exfoliation process, the samples were washed and dried according to the previous experiments. The product had a yield of about 3 wt% [33]

2.3. Synthesis of Silver nanoparticles (Ag.NPs)

AgNPs were produced from cashew leaf extract. The cashew leaves were sourced from Caritas University in the Enugu, Nigerian. 200 g of the leaves were cleaned thoroughly in water and dried in the oven at a temperature of 120°C for 2 hours. 100 ml of ethanol was added to the leaves and allowed to stand for 1 hour, after which the extract was taken and 100 ml of Silver Nitrate (AgNO₃) added. The addition of AgNO₃ to

the cashew leaf extract samples resulted in colour change from the yellow to a dark brown. The reaction mixture was allowed to stand for 30 minutes before it was heated in an electric oven to 100°C while stirred at 2000 rpm. After heating, the solution was centrifuged for 1 hour to yield silver nanoparticles.



Figure 2: Photographs of Cashew leaves

2.4. Design of experiments for composite fabrication

The experiment was designed using the Taguchi experiment design. Taguchi's parametric design approach provides a systematic and efficient method for determining near-optimal design parameters. In this study, each parameter was assessed at three levels. Table 1 summarizes the number of process parameters and their level values. The parameter values and levels were chosen to provide a wide enough range to assess the influence of the variables on the attributes. At room temperature, orange juice (OJ) was used as an environmentally friendly reducing agent to change the sizes of silver and graphene nanoparticles (GAg.NPs/Gr.NPs).

Table.1 The process parameters and their values at various levels.

Process parameters	Low (1)	Medium (2)	High (3)
Gr.NPs(%)	2.5	5.0	7.5
GAg.NPs(%)	0.5	1.0	1.5
Orange juice (OJ)ML	2	4	6
Curing Temperature(°C)	60	80	100

The L9 orthogonal array was formed using the Taguchi technique since we are evaluating four components with three levels each.

2.5. Development of Nanocomposite Samples

The Gr.NPs were functionalized before sample generation. The Gr.NPs were dispersed in orange juice for 30 minutes using an ultrasonic bath sonicator: the act of delivering sonic energy to agitate the particles, then precise amounts of the GAg.NPs were added [35]. In the experiment, orange juice was used both as a reducing agent and as a reaction medium. The suspension was sonicated for 30 minutes to produce a stable brown colloidal solution. The reaction was then stirred magnetically for 10 hours at 60°C. hybrid composites was formed using the process parameters listed in Table 2, and the nanocomposites were formed using a modified solution casting process. The composite panels were made using a wooden mould. After setting, petroleum jelly was applied to facilitate the removal of the composite from the mould. Before reinforcement, 2% cobalt naphthalene (as an accelerator) was fully incorporated into the polyester resin. In addition, follow-up therapy was used to improve particle-matrix interactions. Taguchi's design and Gray's relationship analysis were used to developing the composite for maximum performance. The Taguchi Matrix answers were the performance of the Gr combination.NP, GAg.NP, orange juice (OJ) and ripening temperature. The data were analyzed after conducting test experiments on dielectric constant, capacitance and electrical conductivity. The results obtained were converted into S/N ratio values. Table 2: Experimental Design layout for Nanocomposites Fabrication

Gr.NPs	Gag.NPs	Orange juice	Temperature
1	1	1	1
1	2	2	2
1	3	3	3
2	1	2	3
2	2	3	1
2	3	1	2
3	1	3	2
3	2	1	3
3	3	2	1
Control			

2.6. Determination of the electrical Properties of the developed nanocomposites.

The KAISE Insulation Test (SK5010) was used to measure electrical conductivity, capacitor, and dielectric constant. The samples were tested by sandwiching them between two electrodes. By adjusting the frequency

from 103 to 106Hz, the electrical conductivities and dielectric constants were calculated. Equation 1 was used to calculate the electrical conductivities of the developed composites.

$$\sigma = \frac{1}{\rho} = \frac{d}{(R_p)A} \quad (1)$$

The dielectric constant was computed from Equation 2.

$$\epsilon^1 = \frac{C_p(A)}{A(\epsilon_0)} \quad (2)$$

where: A is the area, d is the thickness, Cp= the capacitance, ϵ_0 =dielectric constant of free space, and ρ =electrical resistivity.

2.7. Scanning Electron Microscope (SEM) analysis

The microstructure of composite materials was investigated using a VEGA 3 TESCAN field emission gun scanning electron microscope (FEG-SEM) at an accelerating voltage of 1-1.5 kV and a working distance of 2.1 mm (Figure 3). Images of the samples, which were shot under high vacuum conditions, were captured using a secondary electron detector. Because of their great electrical conductivity, the samples were scanned without sputtering metal onto their surfaces. The energy-dispersive X-ray spectroscopy (EDS) experiment used a 5 kV accelerating voltage and a working distance of 8.4 mm.



Figure 3: Photograph of SEM/EDS instrument for the analysis of the microstructures of the developed nanocomposites [30]

2.8. Diffractometry Studies using X-Rays (XRD)

The diffraction patterns of nanoparticles and nanocomposites were determined using an X'Pert Pro model diffractometer (XRD). The samples were properly sized and shaped on the device before being evaluated at a 30 kV acceleration voltage and 40 mA current. Cu K radiation was used to scan the surface of the materials under inquiry from $2\theta = 0$ to 90° at a speed of $5^\circ/\text{min}$. Finally, the results were examined using the high score and the XRD software tool. The XRD data were used to approximate the crystallite size of the peaks using the Scherrer equation in the high score algorithm for accuracy based on Equation 3.7.

$$\tau = \frac{K\lambda}{\beta \cos \theta} \quad (3)$$

Where (m) represents the size of ordered domains (crystallite size), (1.54), K represents the form factor (Scherrer constant) set to 0.9, and (radian) represents the full-width half maximum (FWHM).

2.9. Fourier-transform infrared (FTIR) spectroscopic Analysis

The FTIR equipment was used to determine the functional groups of the nanocomposites (Figure 4). This work uncovered the interplay between nanoparticles and modifiers. The research was carried out in the 500-4500 cm⁻¹ wavenumber range. The method was done in attenuated complete reflection mode with a modest noise effect to achieve satisfactory results.



Figure 4: Photograph of FTIR equipment for the analysis of the compositions of the developed nanocomposites [29].

2.10. Thermogravimetric Analyzer (TGA) Analysis

In this investigation, the TA instrument Q500 (Figure 5) was used. TGA measures how a material's physical and chemical properties change with temperature and time. It calculated how much weight the nanocomposites lost as the temperature increased. To avoid sample oxidation or side reactions, the analysis was carried out in an inert atmosphere using nitrogen gas at a rate of 40 mL/min. The analysis was carried out on a sample size of roughly 10 mg at a heating rate of 10 °C/min from 50 °C to 550 °C.



Figure 5: Photograph of DTA-TGA equipment for the analysis of the thermal properties of the developed nanocomposites[28].

2.11. Determining tensile strength

The nanocomposites' tensile strength was determined using a computerized universal testing machine and the ASTM D 3039-76 criteria at a crosshead speed of 10 mm/min. The samples were cut to 177x20x5 mm in length and a gauge length of 180 mm was marked with a scribe. Maximum stress (ultimate tensile strength) and strain were measured.

2.12. Impact energy determination

The Charpy impact tester used in this work is an Instron CEAST 9050 model. It offers information on a material's impact toughness under dynamic load. The experiment was conducted at room temperature with a sample size of 80 x 10 x 4 mm. The sample was clamped onto the sample holder, which had a support span of 62 mm. Following that, the samples were struck with a pendulum harmer hanging at a 150° angle. The intensity of the sample's influence was measured. For each sample, the procedure was done three times. These results represent the average of three tests performed on each sample following ISO 179

3.0 Results and Analysis

3.1 Electrical Properties of the Developed Composites

The electrical properties of the proposed nanocomposite samples were evaluated using the KAISE Insulation Tester (model SK5010). Table 3 displays the generated data.

Table 3: Electrical Properties of the developed composites

Gr.NPs	GAg.NPs	Orange juice	Temperature	thermal conductivity $\text{Wm}^{-1}\text{K}^{-1}$	dielectric constant	electrical conductivity S/m
1	1	1	1	0.9	5.94	9.78E-09
1	2	2	2	1.3	5.45	8.81E-09
1	3	3	3	1.4	4.56	8.67E-12
2	1	2	3	0.9	5.34	9.52E-12
2	2	3	1	1.4	5.67	5.56E-09
2	3	1	2	1.4	4.35	2.54E-08
3	1	3	2	0.8	3.22	2.05E-08
3	2	1	3	1.3	3.56	2.34E-09
3	3	2	1	0.9	5.81	2.54E-09
Control				0.84		

Graphene-polyester nanocomposites are novel materials that exhibit unique electrical properties due to the incorporation of graphene nanoplatelets into the polyester matrix. Graphene is a one-atom-thick layer of graphite with exceptional electrical conductivity, which makes it an attractive material for use in composite materials. The electrical properties of the developed nanocomposites were tuned by varying the concentration and dispersion of graphene within the polyester matrix. The addition of graphene nanoplatelets to the polyester matrix significantly increased the electrical conductivity of the composite. This is due to the high intrinsic electrical conductivity of graphene combined with its large surface area, which allowed for efficient electron transport through the material. The developed nanocomposite also exhibited a high dielectric constant, which is a measure of the material's ability to store electrical energy. The dielectric constant of the composite was tuned by varying the concentration and dispersion of graphene within the matrix. This property makes graphene-polyester nanocomposites useful for applications such as capacitors and energy storage devices.

The electrical conductivity of the graphene/polyester nanocomposite is influenced by several factors, including the concentration and size of graphene particles, the quality of graphene dispersion, and the type of polymer used. The electrical conductivity of the developed nanocomposite increased as graphene concentration increased, resulting in a percolation threshold where a continuous conductive network was formed. The size of graphene particles impacted the electrical conductivity. Smaller particles are known to exhibit higher conductivity because they provide a greater surface area for electron transfer. The quality of graphene dispersion in the polymer matrix also played a significant role in the electrical conductivity of the nanocomposite. Poor dispersion of graphene particles hinders the formation of a continuous conductive network, leading to decreased conductivity.

3.2 TEM image of the Green synthesized AgNP

The size and shape of the AgNPs were evaluated using TEM. Figure 6 shows the results of the TEM imaging of the synthesized AgNPs. The microstructure shows spherical and circular forms, as well as well-distributed nanoparticles with no clumping. The particle size ranged from 25 to 45 nanometers.

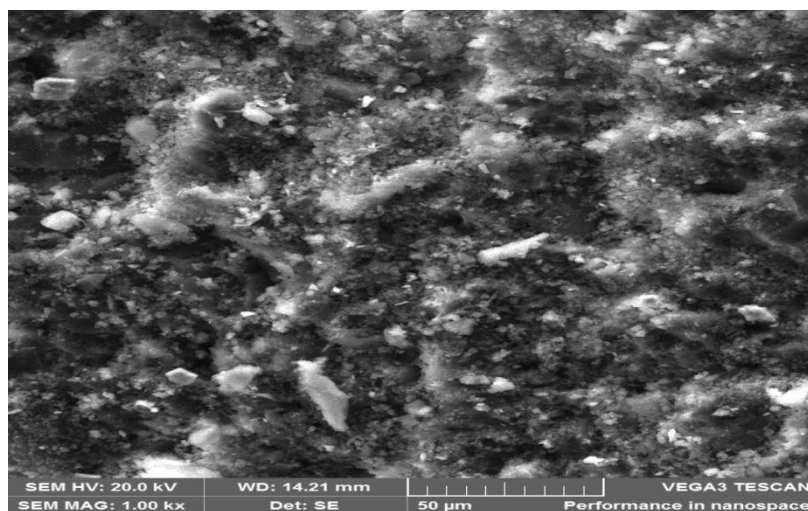


Figure 6: Transmission electron microscopy image of AgNPs

3.3 TEM image of the developed Graphene from rice husk

Transmission electron microscopy (TEM) is a high-resolution imaging technique used to observe the structural details of nano-scale materials. Graphene made from rice husks is a novel material synthesized from the agricultural waste of rice husks. The TEM image of graphene made from rice husk shows a thin and transparent black sheet-like structure consisting of closely packed hexagonal-shaped carbon atoms. The graphene sheets are highly uniform in thickness and size, with a thickness of around one atom. The edges of the graphene sheets appear smooth and well-defined, indicating high-quality material. The TEM image also shows the presence of defects in the form of pores and wrinkles, which are natural occurrences in graphene sheets. Overall, the TEM image of graphene made from rice husk reveals a unique and promising material for various applications in electronics, energy, and other fields.

(Figure 7). Carbon exhibits the strongest peaks in all materials under evaluation, according to the EDS spectra (Figure 8). It was observed that the graphene planes become parallel to the incident electron beam and appear in the TEM image due to the structural properties of graphene, which allow it to adsorb specific molecules and electrostatic interactions, improving electronic, electrochemical, and/or optical signal measurement selectivity and sensitivity.

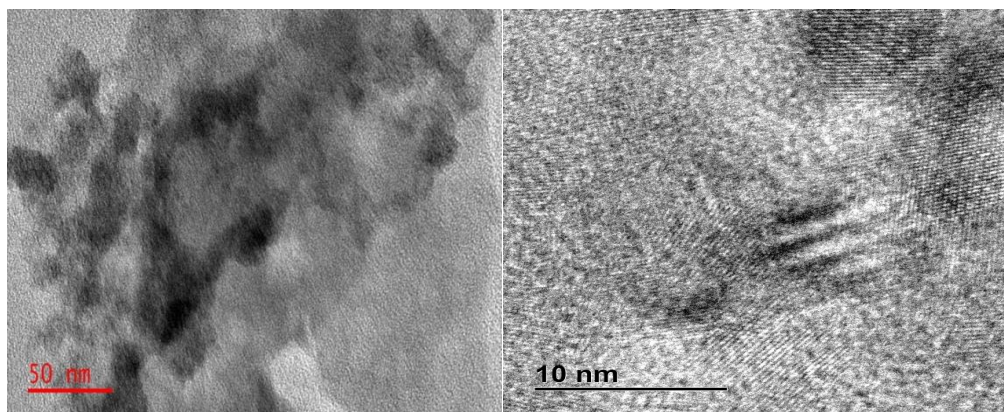


Figure 7 Transmission electron microscopy image of graphene at 50 and 10nm respectively



Figure 8: Energy-dispersive X-ray spectroscopy analysis image of graphene

3.4 TEM images of Modified Ag.NPs on Graphene(Gr)

Figure 9 shows a TEM image of blended Gr with Ag.NPs composite. There was no evidence of agglomeration between the Gr and AgNPs. The particles were uniformly and effectively disseminated because both AgNO_3 and GO are oxidizing agents, which interestingly confirmed the occurrence of Ag.NPs on the graphene composite nanosheets. Instead of reacting with one another, they preferentially reacted with the reducing agent, resulting in the deposition of Ag.NPs on the surface of graphene nanosheets.

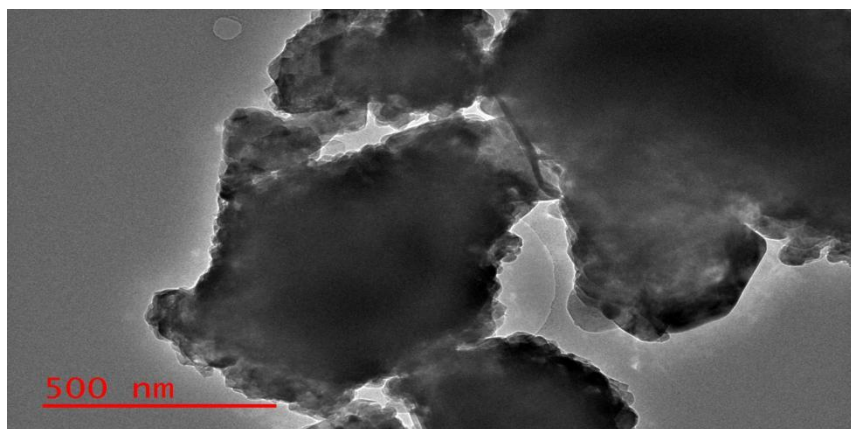


Figure 9: Transmission electron microscopy image of Modified Ag.NPs on Graphene(Gr) surface

3.5 Microstructure Analysis

The microstructure consists of a polymer matrix made of polyester with evenly dispersed graphene particles derived from rice husk. The nanocomposite has a homogenous distribution of graphene particles throughout the matrix, creating a strong and rigid material. The graphene particles, derived from rice husk, have a sheet-like structure composed of carbon atoms bonded together in a hexagonal lattice. The particles are typically 50 nanometers in size. The graphene had a high surface area for interaction with the polyester matrix, allowing for a good bond between the two materials, and enhancing the mechanical properties of the nanocomposite.

The SEM images of polyester and the developed nanocomposites are shown in Figures 10 and 11. SEM analysis shows that graphene particles are homogeneously distributed in the polyester matrix, indicating good dispersion and uniform mixing of the graphene particles. It revealed that graphene particles are tightly adhered to the polymer matrix, suggesting that the addition of graphene enhanced the interfacial bonding between the polymer matrix and the graphene particles. The SEM images indicated that graphene particles are dispersed in a single layer or a few-layer form, which reduced the agglomeration and ensures more efficient filler dispersion. It depicted an increase in the surface roughness of the nanocomposite material, which suggests that the addition of graphene particles changed the surface morphology of the polyester matrix. SEM analysis shows that the addition of graphene increased the stiffness and strength of the nanocomposite material by utilizing the strong mechanical properties of graphene. It also suggested that the

addition of graphene decreases the porosity of the nanocomposite, indicating improved barrier properties and reduced water absorption.

There was a substantial contrast between the SEM pictures of polyester and the composites. White phases highlighted the reinforcements, with the presence of Ag.NPs. The decorated samples had a uniform and even dispersion of Ag.NPs. The inclusion of Ag.NPs and orange juice aided in the modification of the network structure of Gr.NPs, resulting in better interfacial bonding between the polymer and the reinforcement. Previously [32]. In the absence of Ag.NPs and orange juice, small agglomerates and segregation of Gr.NPs were obtained, which impacted electrical conductivity and dielectric constants. The silver nanoparticles helped and strengthened interfacial polarization and high dielectric constant, as well as maintaining established conducting routes, to produce polymer composites with higher dielectric constants.

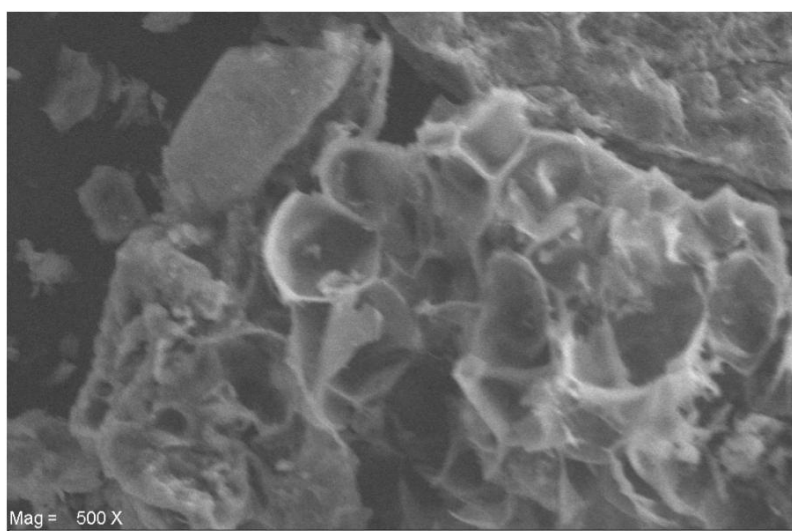


Figure10: Scanning electron microscope analysis image of the developed polyester/7.5%Gr/NPs-0.5%Ag. NPs/4ml orange juice nanocomposite

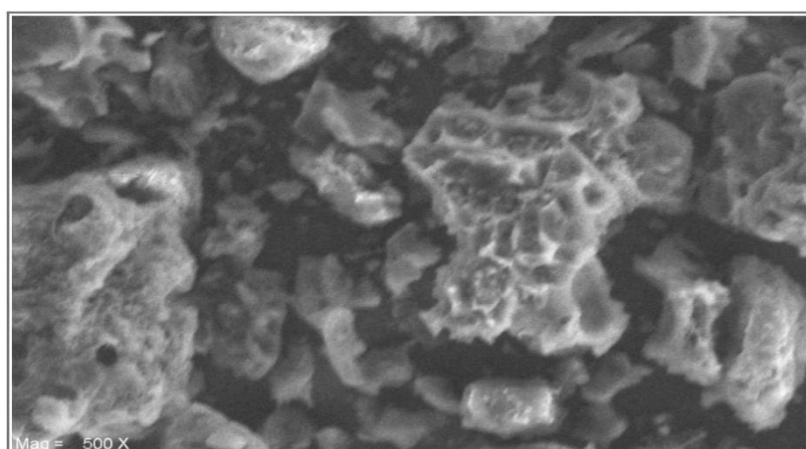


Figure 11: Scanning electron microscope analysis image of polyester/7.5%Gr. NPs composites

3.6 Mechanical analysis of polyester and the developed composites

Table 4, shows the mechanical properties of the developed composites.

Table 4. Results of mechanical properties analysis of the developed nanocomposites.

Samples	EM (MPa)	YS (MPa)	TS (MPa)	EB (N.M)	ELB (mm)
polyester-matrix	1300.7	50.833	51.667	0.049	4.286
polyester-7.5%Gr.NPs-0.5%Ag.NPs	1961.491	97.778	98.333	0.195	9.994
polyester-7.5%Gr.NPs	1323.453	55.0	55.278	0.062	5.683

EM is for elastic modulus, YS stands for yield strength, TS stands for tensile strength, EB stands for energy at the break, and ELB stands for elongation at the break.

The addition of graphene nanoplatelets (GrNPs) to the polyester matrix can significantly improve its modulus from 1300.7 to 1961.5 MPa. The elastic modulus is influenced by the dispersion and alignment of GrNPs, as well as the matrix-filler interface bonding. The high aspect ratio of GrNPs provides a large surface area for matrix-filler interaction, enhancing the stiffness of the nanocomposite.

Research studies have reported that the elastic modulus of graphene-polyester nanocomposites can be improved by up to 85% compared to the neat polyester matrix. The increase in modulus with GrNPs loading can be attributed to the formation of a percolated network of GrNPs, which effectively transferred load between individual particles through the matrix. Moreover, the high modulus and strength of graphene reinforced the polymer matrix, resulting in improved moduli, enhanced stiffness and mechanical strength of the material.

Graphene-polyester nanocomposites were found to exhibit improved tensile strength compared to pure polyester. The tensile strength of a material refers to its ability to withstand stretching or tension without breaking. When graphene was added to the polyester matrix, it formed a strong interfacial bond, thereby reinforcing the material and increasing its tensile strength. Several studies had reported significant improvements in tensile strength with the addition of graphene to polyester composites. For example, [6] found that the tensile strength of polyester composites increased by up to 128% when graphene was added in small amounts. Another study [7] observed a 115% increase in tensile strength when a small amount of graphene was added to a polyester matrix.

The improved tensile strength of graphene-polyester nanocomposites is attributed to several factors. Firstly, graphene had a high aspect ratio, which conferred a large surface area for interaction with the polymer matrix, and facilitated strong interfacial bonding between the graphene and the polyester, leading to the reinforcement of the material. Additionally, graphene is a highly mechanical and durable material, which

helped to prevent cracks and fractures in the composite structure. Finally, the graphene-polyester nanocomposite exhibited uniform distribution of the polymer chains, which helped to prevent weak spots and defects that may occur in pure polyester. The higher tensile strength and elastic modulus of the polyester-7.5%Gr.NPs and polyester-7.5%Gr.NPs +0.5%Ag.NPs nanocomposite demonstrates that the reinforcing phases were successful in enhancing the strength of the polyester matrix (Table 4). The polyester-7.5%Gr.NPs +0.5%Ag.NPs sample had the highest tensile strength of all samples, with tensile strengths of 50.833, 55.00, and 97.778 MPa obtained for the polyester-matrix, polyester-7.5%Gr.NPs, and polyester-7.5%Gr.NPs +0.5%Ag.NPs, respectively, correspond to a 92.35 per cent increase in the tensile strength of pure polyester.

The yield strength property of graphene-polyester nanocomposite refers to the maximum stress that the composite material can handle before it undergoes permanent deformation or failure. The addition of graphene nanoparticles to the polyester matrix enhances the yield strength of the resulting nanocomposite material. The increase in yield strength is due to the strong interfacial bonding between the graphene nanoparticles and the polymer matrix, which results in a more rigid and stable composite structure. The precise value of the yield strength depends on the specific composition and processing conditions of the nanocomposite material. Researchers have reported yield strengths of graphene-polyester nanocomposites ranging from 63 MPa to 120 MPa, depending on the graphene content, dispersion quality, and other factors. This compares favourably to the value of 97.778 MPa obtained from this work.

The energy at break property of a graphene-polyester nanocomposite is a measure of the materials' strength and ability to resist deformation or failure. Graphene, a two-dimensional material composed of carbon atoms, is known to enhance the mechanical properties of polymers due to its high aspect ratio, exceptional mechanical strength, and high surface area. When graphene is incorporated into a polyester matrix, it forms a nanocomposite material that exhibits improved tensile strength, modulus, and toughness. The energy at break property of the graphene-polyester nanocomposite is therefore improved compared to pure polyester, from 0.049 to 0.195 N.M in this work, making it an attractive material for various applications.

The elongation at break property of graphene-polyester nanocomposite measured the material's ability to stretch or deform before breaking. This property is crucial in determining the toughness and durability of materials used in various applications. The addition of graphene to polyester resulted in an increase in the elongation at break property of the nanocomposite from 4.29 to 10 mm. The presence of graphene improved the interfacial bonding between the polymer and the reinforcement, thereby increasing the material's ability to accommodate deformation without failure. As a result, graphene-polyester nanocomposites exhibited higher strength and toughness compared to pure polyester material, making it suitable for a wide range of applications, including aerospace, automotive, and medical industrial materials.

The stress-strain curves produced from the samples under investigation are shown in Figures 13 to 15. Figures 14 and 15 show that composites have a wider area under the stress-strain curve than pure polyester.

These results suggest that polyester-7.5%Gr.NPs and polyester-7.5%Gr.NPs +0.5%Ag.NPs are both effective. Nanocomposites are more durable and absorb more energy before breakage than pure polyester-based matrices.

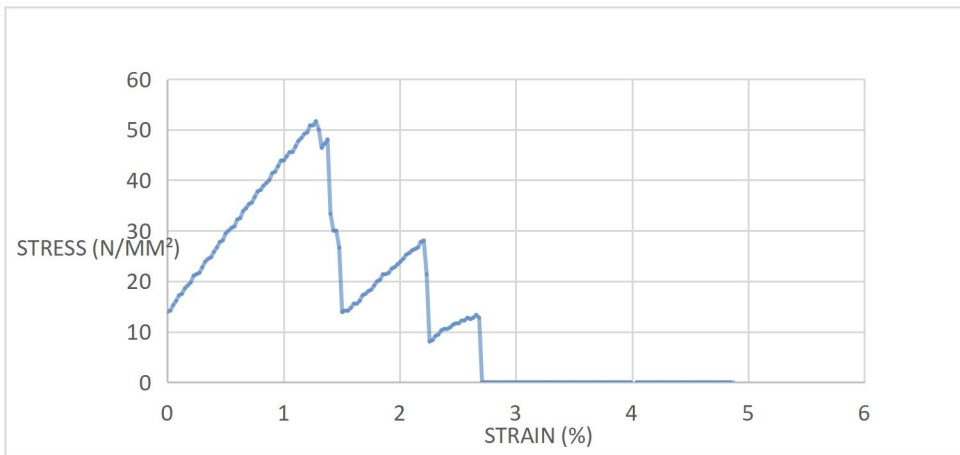


Figure 12: Stress-strain curve of polyester matrix

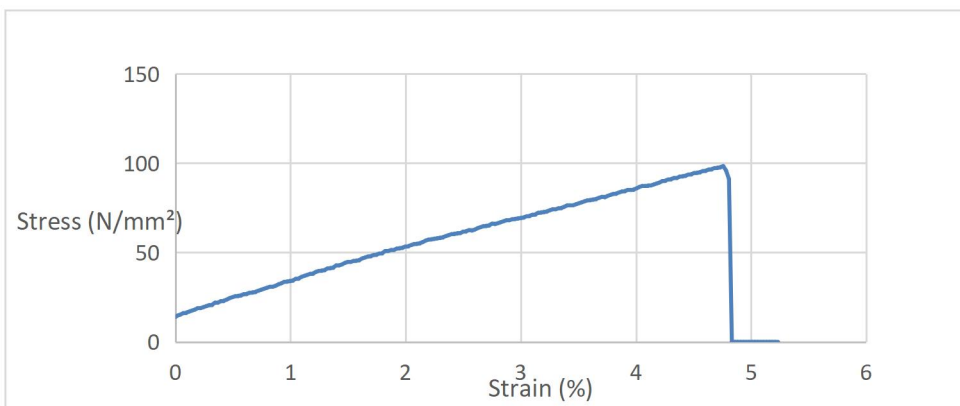


Figure 13: Stress-strain curve of polyester/7.5%Gr.NPs/0.5%Ag.NPs/4ml orange juice nanocomposite

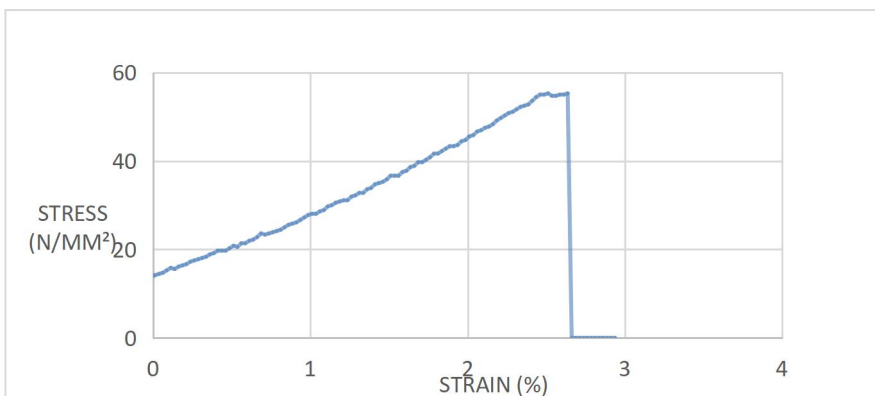


Figure 14: Stress-strain curve of the polyester/7.5%Gr.NPs composites

3.7 XRD Analysis

X-ray diffraction (XRD) is a useful technique for the characterization of nanocomposites, such as graphene-polyester nanocomposites. XRD was used to determine the crystallinity, crystal structure, and orientation of graphene nanosheets in the polyester matrix. The XRD pattern of a graphene-polyester nanocomposite typically showed characteristic peaks at low angles, indicating the presence of intercalated graphene sheets within the polymer matrix. The sharp peak at around $2\theta = 26^\circ$ corresponds to the (002) plane of graphene, which is an indication of the graphene's orientation and interlayer spacing. The intensity of the (002) peak in the XRD pattern of the graphene-polyester nanocomposite is used to estimate the degree of graphene exfoliation and the quality of the nanocomposite. A higher intensity of the (002) peak indicates a higher degree of exfoliation, which is important for maximizing the properties of the nanocomposite.

In addition to the (002) peak, the XRD pattern of graphene-polyester nanocomposites showed additional peaks corresponding to other graphene planes, such as the (100), (101), and (110) planes. These peaks give information about graphene crystallinity, orientation, and quality. The 002 plane of graphene refers to a particular orientation of the carbon atoms in the graphene lattice. In the 002 planes, the carbon atoms are arranged in a hexagonal pattern with two layers of atoms stacked on top of each other. This orientation is important for understanding the electronic and mechanical properties of graphene, as it can affect the way the material interacts with other substances and the way it responds to stress or strain. The 002 plane is one of many possible orientations for graphene, and scientists are exploring different ways to manipulate and engineer the material for a wide range of applications in electronics, energy, and other fields.

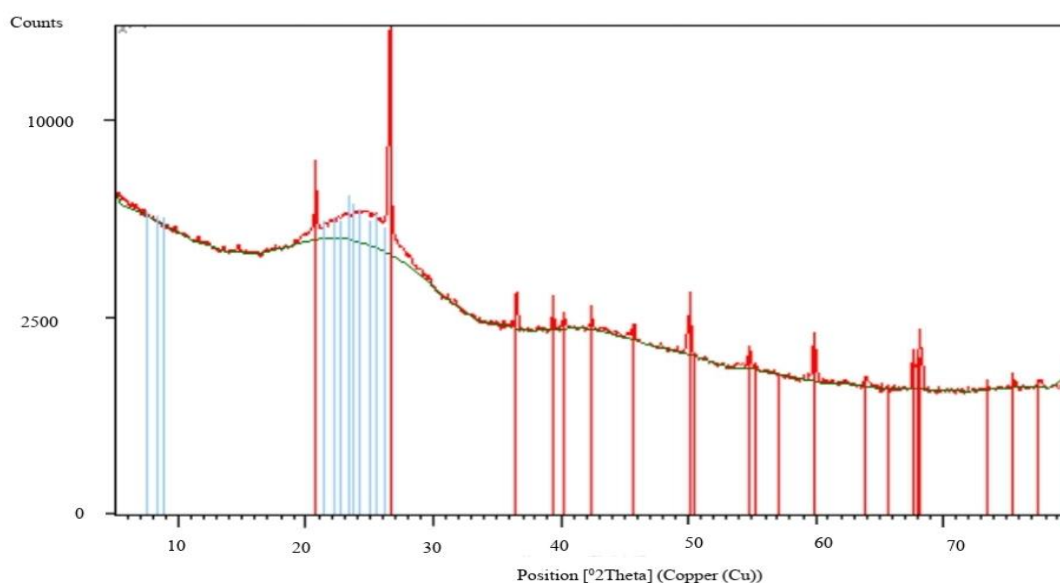


Figure 15: X-ray diffraction analysis of Ag.NPs/4ml orange juice nanoparticle

The crystallinity and phase components of the produced Ag.NPs nanoparticles (Fig.16) were investigated using the XRD pattern. The reflections caused strong peaks in the XRD pattern.

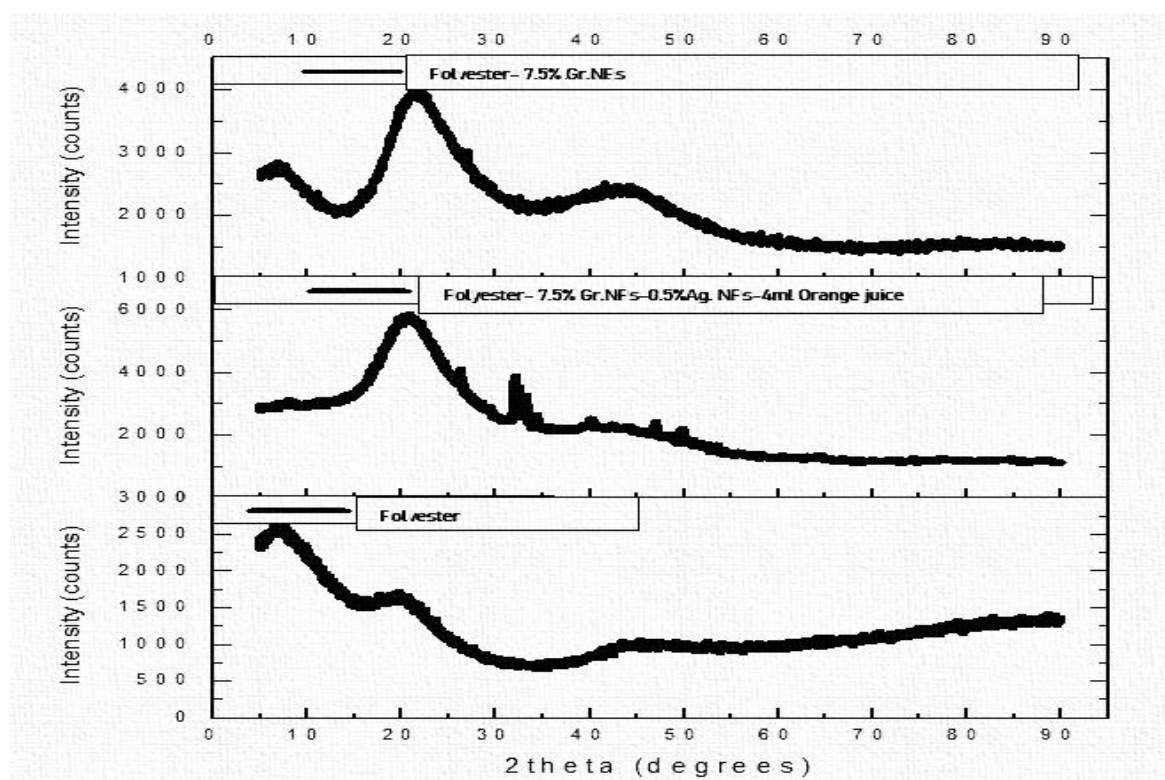
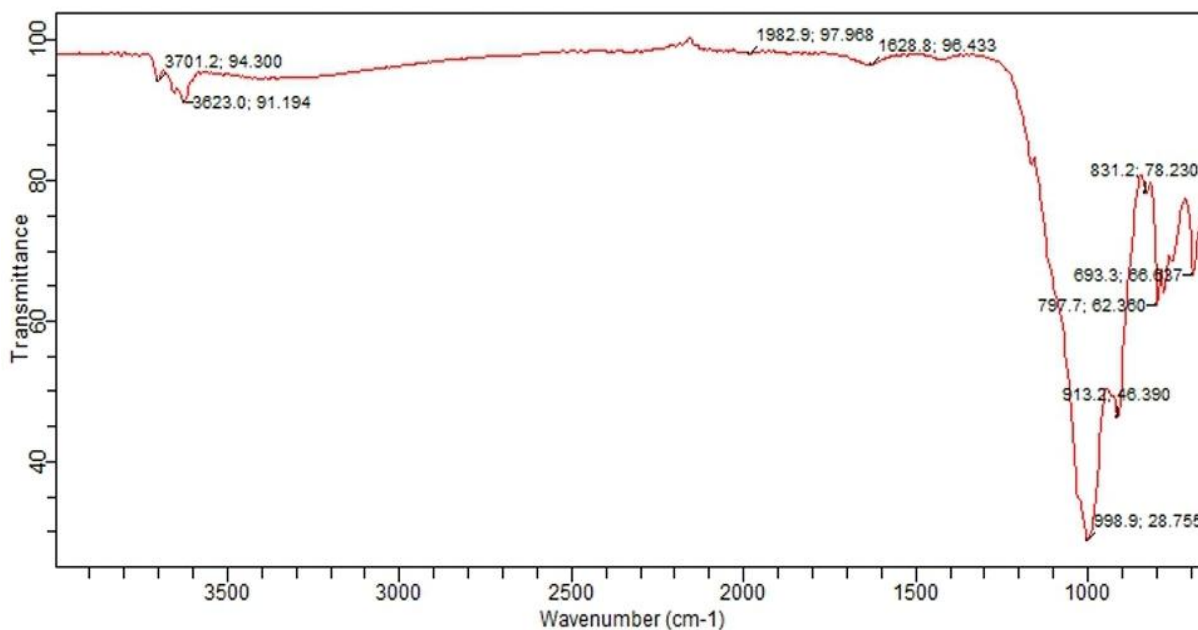


Figure 16: X-ray diffraction analysis pattern of the polyester and the developed nanocomposites.

The XRD spectrum of the X-ray diffraction data of polyester and the produced nanocomposites are shown in Figure 16. The results revealed that the incorporation of Gr.NPs, Ag.NPs and orange juice in polyester had two principal effects: reinforcing and nucleation. The reinforcing action enhanced the crystallinity of the bulk. The addition of the reinforcement to the matrix altered the positions of the distinctive peaks. The inclusion of Gr.NPs-Ag.NPs-4ml orange juice resulted in the discovery of additional peaks in the XRD patterns. This demonstrated a substantial interaction between Gr.NPs-Ag.NPs-4ml orange juice and the polyester matrix. In the XRD, the polymer revealed a broad and less intense band, indicating its semi-crystalline structure. The composites' XRD patterns revealed strong peaks, indicating crystalline structure. The XRD measurements revealed that there were interactions between the reinforcement and the polymer, which strengthened the matrix. The polar groups in the polymers reduced the d-spacing in the composites, resulting in a stronger and denser composite.

3.8 FTIR Analysis of developed composite: Polyester-7.5%Gr.NPs-0.5%Ag.NPs-4ml orange juice



juice

Figure 17: FTIR of Polyester-7.5%Gr.NPs-0.5%Ag.NPs-4ml orange juice composite.

FTIR (Fourier-transform infrared spectroscopy) of the developed graphene-polyester nanocomposite analyzed the chemical groups and bonding present in the material and helped in understanding the interaction between the graphene and the polyester matrix. Figure 17 shows the result of FTIR spectroscopy. This investigated the available surface bonding of the produced nanocomposites. Several active surface bonds were discovered in the FTIR spectrum in the 4,000-400 c/m range, confirming the presence of active functional groups on the surface of the nanocomposite. The detailed description of all the significant peaks observed in the FTIR spectrum bands (c/m) and description of bands include: 3,454 (C=C) stretching; 1,634 (O-H) scissor bending; 1,421 (C=O) bending vibrations; 1,064 (Ag-Ca) stretching; 875 (CH₂) bending vibrations; 712 (Ag-O) stretching; 624 (-COO-) stretching.

The interactions between the graphene and the polyester matrix were observed from changes in the intensity, shape, and position of the peaks. Shifts in the peaks indicated changes in bond strengths due to the bonding between graphene and the polyester matrix. The nanoparticles were well dispersed and interacted strongly with the polyester matrix, as a result of the reduction in intensity

3.9 Thermal properties analysis

Graphene-polyester nanocomposites have excellent thermal conductivity due to the high thermal conductivity of graphene. The addition of small amounts of graphene to polyester significantly enhanced the

thermal properties of the composite material. The high surface area of graphene promoted heat transfer within the material, which lead to faster thermal diffusion and reduced thermal resistance.

Research had shown that the thermal conductivity of graphene-polyester nanocomposites could be increased by up to 400% [16] compared to pure polyester. This enhancement in thermal conductivity was attributed to the strong interfacial interaction between graphene and the polyester matrix, which leads to the effective transfer of heat from the matrix to the graphene filler.

Moreover, graphene-polyester nanocomposites also showed improved thermal stability compared to pure polyester. The presence of graphene prevented the formation of thermal degradation products and the thermal stability of the composite was enhanced, leading to better resistance to heat.

Figures 18 to 20 show the DTA/TGA scan results for the samples. Figure 19 indicated that all of the samples' TGA curves follow a similar trend. Each sample revealed three unique zones. The TGA curves moved to a higher temperature when 7.5% Gr.NPs +0.5%Ag.NPs were added to the polyester. The composites' breakdown is slowed by -7.5% Gr.NPs +0.5%Ag.NPs (Figure 19). This thermal study results revealed that the polyester at the same temperature retained less than 0% of its original weight and that the polyester-7.5%Gr.NPs +0.5%Ag.NPs composites retained more than 15% of their weight at temperatures around 500°C. Figures 19 and 20 shows that the greatest thermal breakdown temperatures for polyester and composites were 350 and 382 °C, respectively. Polyester nearly eliminated char residue at 500 °C. The results indicate that adding 7.5% Gr.NPs +0.5% Ag.NPs to polyester raised the decomposition temperature.

The endothermic effects found in the temperature range mentioned were most likely generated by the links formed in the polymer's backbone, cross-linking of the dehydrogenating polyester macromolecules, and the continuous oxidation of its thermal breakdown byproducts. The 7.5%Gr.NPs +0.5%Ag.NPs reinforced with polyester improved stabilization and raised the temperature of the maximum decomposition/ destruction rate. The maximums of the endothermic peaks shifted to higher temperatures with 7.5%Gr.NPs +0.5%Ag.NPs, showing greater thermal stability of the polymer matrix due to the integration of 7.5%Gr.NPs +0.5%Ag.NPs particles.

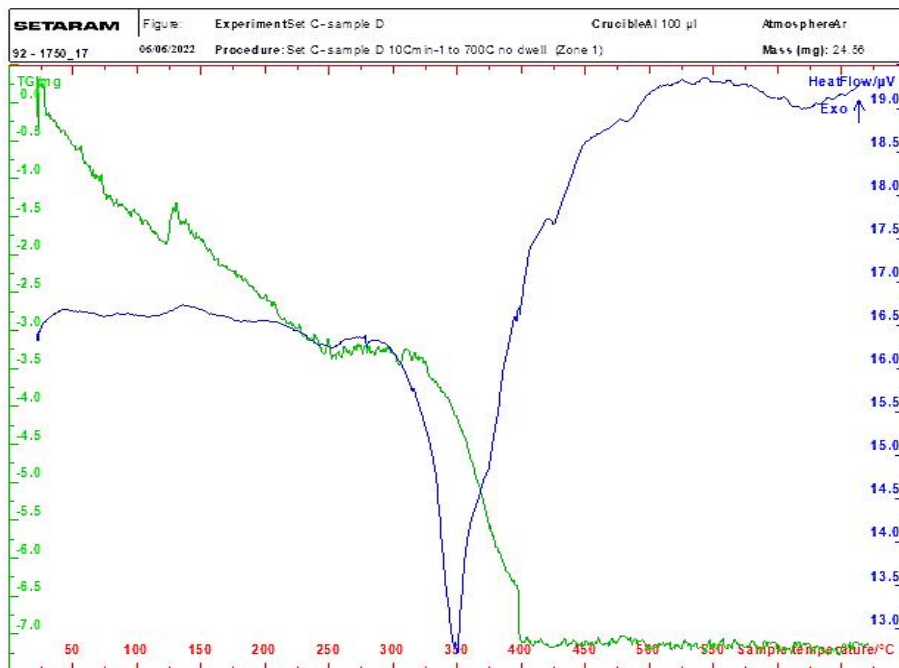


Figure 18 TGA/DTA graph of polyester matrix

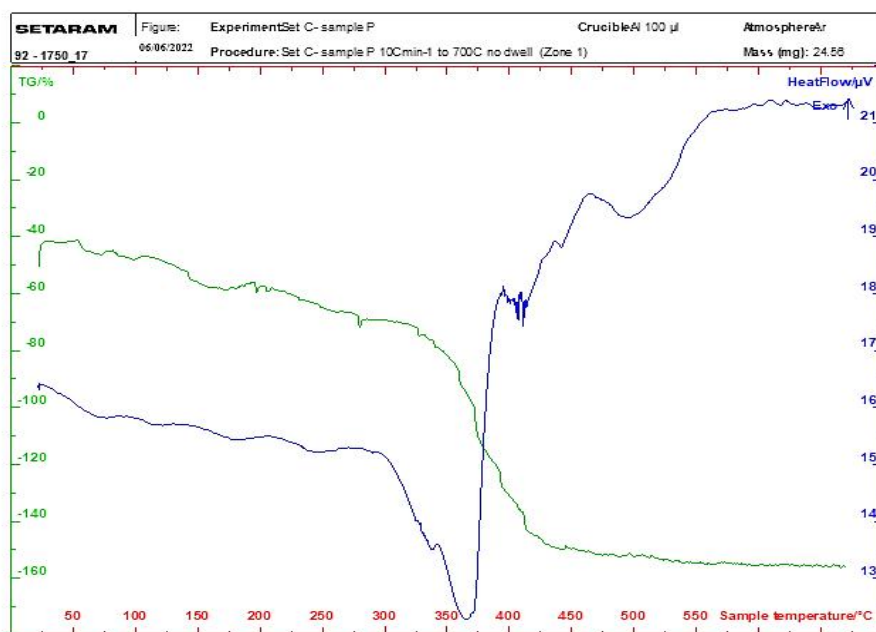


Figure 19: TGA/DTA graph of polyester/7.5%Gr.NPs/0.5%Ag.NPs/4ml orange juice

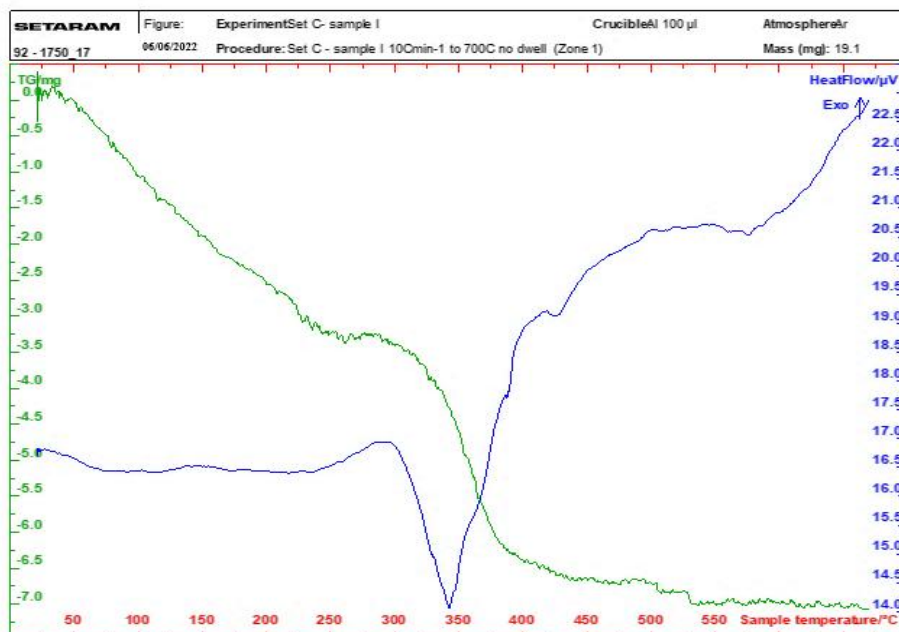


Figure 20: TGA/DTA graph of polyester/7.5%Gr.NPs composites

4.0 Conclusion

The basis of this research work was informed by recent advances in the synthesis of conductive polymers. Environmental concerns and modification of properties to suit a given end use were realised in the application of polyester matrix, green synthesised silver nanoparticles, and graphene derived from rice husks to develop conductive polymers with good experimental conductive potential to replace metals and semiconductors in the electrical and electronic industry. Since the silver nanoparticle-doped polyester matrix had electrically conductive properties and could store positive charges in the polymer chain, it would serve as a good polymer conductor for the creation of conductive engineering materials. A polyester nanocomposite reinforced with Gr.NPs and doped with Ag.NPs and orange juice were successfully synthesised utilising the solution stir cast process. The high electrical, and thermal conductivity and dielectric constants obtained at optimal conditions were a result of the high electron mobility of Ag.NPs-Gr.NPs enhanced the conductivity of polyester. The electrical conductivity of $2.08 \times 10^{-8} \text{ S/m}$, and the dielectric constant of 5.95. and thermal conductivity of $1.45 \text{ Wm}^{-1}\text{K}^{-1}$, obtained for optimal conditions are adequate for microelectronic and semiconductor devices manufacture. A 92.35 per cent increase in tensile strength of the pure polyester was obtained in comparison to polyester-7.5 %Gr. NPs +0.5%Ag. NPs.

Waste rice husk is suitable for use in the development of graphene nanoparticles for the production of conductive polymers. It was established that Ag.NPs synthesized using cashew leaf extract as a reducing agent enhanced good dispersion of Gr.NPs for the production of conductive polymer. Orange juice has been confirmed as an adequate replacement for vitamin C (ascorbic acid) and as a nontoxic reducing agent dimensions control of Ag.NPs on Gr.NPs. The developed composite is suitable for application in the production of microelectronic devices and conductive polymers. Graphene-polyester nanocomposites have the potential to revolutionize the electrical engineering industry by providing a range of advanced properties

that can be leveraged in a variety of applications. Graphene when combined with polyester, resulted in a nanocomposite that would conduct electricity more efficiently than traditional materials. This property can be used in applications such as wires, cables, and electrical connectors. By incorporating graphene into polyester, the resulting nanocomposite provided better thermal management in electrical systems, which could be applied to reducing the risk of overheating and damage. Polyester is a durable and flexible material, but it can benefit from the addition of graphene, which increased its strength and resilience. This property can be leveraged in various electrical applications such as protective coatings, high-strength composites, and structural materials for electrical components. Overall, the use of graphene-polyester nanocomposites in the electrical engineering industry can result in innovative materials with enhanced properties that can benefit a range of applications.

Competing interest

The author declare that they have no known competing financial interests or personal relationships that could have appeared to influence the work reported in this paper

Funding

The author received no funding for this study.

Acknowledgements

This work received administrative support from the Department of Chemical Engineering, Caritas University Enugu, Nigeria.

List of Abbreviations

CNTs –Carbon nanotubes
 Gr.NPs -Graphene nanoparticles
 Ag.NPs -Silver nanoparticles
 MEK -Methyl-ethyl-ketone
 RH -Rice husk
 CRH -Carbonizes rice husk
 KOH -Potassium hydroxide
 SCCM -Standard cubic centimetres per minute
 NaOH -Sodium hydroxide
 OJ -Orange juice
 SEM -Scanning electron microscope
 EDS -Energy dispersion spectroscopy
 XRD -X-ray diffractometer
 FWHM -Full width half maximum
 FTIR -Fourier transform infrared
 TGA -Thermogravimetric analyzer
 Gr -Graphene
 TEM -Transmission electron microscope
 ISO -International standards organization
 ASTM -American society for testing and materials

References

- [1] E.M. Ezech, O.D. Onukwuli, R.S. Odera, Novel flame-retarded polyester composites using cow horn ash particles, *Int. J. Adv. Manuf. Technol.* 103 (2019). <https://doi.org/10.1007/s00170-019-03678-2>.
- [2] D.G. Papageorgiou, I.A. Kinloch, R.J. Young, Mechanical properties of graphene and graphene-based nanocomposites progress in materials science mechanical properties of graphene and graphene-based nanocomposites, *Prog. Mater. Sci.* 90 (2017).
- [3] M. Azizi-Lalabadi, S.M. Jafari, Bio-nanocomposites of graphene with biopolymers; fabrication,

- properties, and applications, *Adv. Colloid Interface Sci.* 292 (2021). <https://doi.org/10.1016/j.cis.2021.102416>.
- [4] Y. Xiang, L. Xin, J. Hu, C. Li, J. Qi, Y. Hou, X. Wei, Advances in the applications of graphene-based nanocomposites in clean energy materials, *Crystals*. 11 (2021). <https://doi.org/10.3390/cryst11010047>.
- [5] R. Sun, L. Li, H. Zhang, J. Yang, Effect of hydrogen functionalization on interfacial behavior of defective-graphene/polymer nanocomposites, *Polym. Compos.* 41 (2020). <https://doi.org/10.1002/pc.25454>.
- [6] H.B. Kulkarni, P. Tambe, G. M. Joshi, Influence of covalent and non-covalent modification of graphene on the mechanical, thermal and electrical properties of epoxy/graphene nanocomposites: a review, *Compos. Interfaces*. 25 (2018). <https://doi.org/10.1080/09276440.2017.1361711>.
- [7] U. Szeluga, S. Pusz, B. Kumanek, K. Olszowska, A. Kobylukh, B. Trzebicka, Effect of graphene filler structure on electrical, thermal, mechanical, and fire retardant properties of epoxy-graphene nanocomposites - a review, *Crit. Rev. Solid State Mater. Sci.* 46 (2021). <https://doi.org/10.1080/10408436.2019.1708702>.
- [8] M. Muthu Meenakshi, G. Annasamy, M. Sankaranarayanan, Green synthesis of graphene gold nanocomposites for optical sensing of ferritin biomarker, *Mater. Lett.* 303 (2021). <https://doi.org/10.1016/j.matlet.2021.130446>.
- [9] E. George, J. Joy, S. Anas, Acrylonitrile-based polymer/graphene nanocomposites: A review, *Polym. Compos.* 42 (2021). <https://doi.org/10.1002/pc.26224>.
- [10] H. Yao, L.P. Wu, G.Q. Chen, Synthesis and Characterization of Electroconductive PHA- graft- Graphene Nanocomposites, *Biomacromolecules*. 20 (2019). <https://doi.org/10.1021/acs.biomac.8b01257>.
- [11] R.R. Santhapuram, S.E. Muller, A.K. Nair, Nanoscale bending properties of bio-inspired Ni-graphene nanocomposites, *Compos. Struct.* 220 (2019). <https://doi.org/10.1016/j.compstruct.2019.03.093>.
- [12] J. Payandehpeyman, M. Mazaheri, M. Khomehchi, Prediction of electrical conductivity of polymer-graphene nanocomposites by developing an analytical model considering interphase, tunnelling and geometry effects, *Compos. Commun.* 21 (2020). <https://doi.org/10.1016/j.coco.2020.100364>.
- [13] C.J. Akinyi, J.O. Iroh, Heat of decomposition and fire retardant behaviour of polyimide-graphene nanocomposites, *Energies*. 14 (2021). <https://doi.org/10.3390/en14133948>.
- [14] K. Bilisik, M. Akter, Graphene nanocomposites: A review on processes, properties, and applications, *J. Ind. Text.* (2021). <https://doi.org/10.1177/15280837211024252>.
- [15] A. Allahbakhsh, F. Noei Khodabadi, F.S. Hosseini, A.H. Haghighi, 3-Aminopropyl-triethoxysilane-functionalized rice husk and rice husk ash reinforced polyamide 6/graphene oxide sustainable nanocomposites, *Eur. Polym. J.* 94 (2017). <https://doi.org/10.1016/j.eurpolymj.2017.07.031>.
- [16] N. Fatimah, T. Arifin, N. Yusof, A. Fauzi Ismail, J. Jaafar, F. Aziz, W. Norhayati, W. Salleh, Graphene from waste and bioprecursors synthesis method and its application: A review, 2020.
- [17] N. Dutta, T.K. Maji, Development of waste rice husk/PVC/GO nanocomposite using TA–CaO adduct and ESO as green additives, *J. Thermoplast. Compos. Mater.* (2022). <https://doi.org/10.1177/08927057211063398>.
- [18] T. Ouyang, J. Tang, F. Liu, C.-T. Chang, Preparation of Graphene Oxide Modified Rice Husk for Cr(VI) Removal, *J. Nanosci. Nanotechnol.* 19 (2019). <https://doi.org/10.1166/jnn.2019.16662>.
- [19] I. Rhee, J.S. Lee, J.H. Kim, Y.A. Kim, Thermal performance, freeze-and-thaw resistance, and bond strength of cement mortar using rice husk-derived graphene, *Constr. Build. Mater.* 146 (2017). <https://doi.org/10.1016/j.conbuildmat.2017.04.109>.
- [20] A.A. Yekinni, M.O. Durowoju, J.O. Agunsoye, L.O. Mudashiru, L.A. Animashaun, O.D. Sogunro, Automotive Application of Hybrid Composites of Aluminium Alloy Matrix : A Review of Rice Husk Ash Based Reinforcements, *Int. J. Compos. Mater.* 9 (2019).
- [21] F.E. Che Othman, N. Yusof, A.F. Ismail, J. Jaafar, W.N. Wan Salleh, F. Aziz, Preparation and characterization of polyacrylonitrile-based activated carbon nanofibers/graphene (gACNFs) composite synthesized by electrospinning, *AIP Adv.* 10 (2020). <https://doi.org/10.1063/5.0008012>.
- [22] T.H. Liou, Y.K. Tseng, S.M. Liu, Y.T. Lin, S.Y. Wang, R.T. Liu, Green synthesis of mesoporous graphene oxide/silica nanocomposites from rich husk ash: Characterization and adsorption performance, *Environ. Technol. Innov.* 22 (2021). <https://doi.org/10.1016/j.eti.2021.101424>.
- [23] O.F. Abraham, V.S. Aigbodion, E.C. Ejiogu, U.C. Ogbuefi, Rice husk derived graphene and zinc oxide composite anode for high reversible capacity lithium-ion batteries, *Diam. Relat. Mater.* 123

- (2022). <https://doi.org/10.1016/j.diamond.2022.108885>.
- [24] R.J. Ramalingam, H. Al-Lohedan, A.M. Tawfik, G. Periyasamy, M.R. Muthumareeswaran, Synthesis and characterization of mos2 –grapene oxide on ni-co-mno2 nanofiber like binary composite for nickel foam based flexible electrode fabrication, Chalcogenide Lett. 17 (2020).
- [25] A.T. Smith, A.M. LaChance, S. Zeng, B. Liu, L. Sun, Synthesis, properties, and applications of graphene oxide/reduced graphene oxide and their nanocomposites, Nano Mater. Sci. 1 (2019). <https://doi.org/10.1016/j.nanoms.2019.02.004>.
- [26] A. Naskar, S. Bera, R. Bhattacharya, P. Saha, S.S. Roy, T. Sen, S. Jana, Synthesis, characterization and antibacterial activity of Ag incorporated ZnO-graphene nanocomposites, RSC Adv. 6 (2016). <https://doi.org/10.1039/c6ra14808e>.
- [27] I.A. Ovid'ko, Enhanced mechanical properties of polymer-Matrix nanocomposites reinforced by graphene inclusions: A review, Rev. Adv. Mater. Sci. 34 (2013).
- [28] O. O.D, E.M. Ezech, Assessment of the fire retardant effect potential of carbonized cow horn ash additive in banana peduncle fibre reinforced polyester composites, World J. Eng. (2021). <https://doi.org/10.1108/WJE-07-2021-0438>.
- [29] E.M. Ezech, O.D. Onukwuli, Comparative Cone calorimetric analysis of the fire retardant properties of natural and synthetic additives in banana peduncle fibre reinforced polyester composites, Moroccan J. Chem. 9 (2021). <https://doi.org/10.48317/IMIST.PRSM/morjchem-v9i3.21954>.
- [30] E.M. Ezech, O.D. Onukwuli, Physicochemical characterization of cow horn ash and its effect as filler material on the mechanical property of polyester-banana fibre composite, World J. Eng. 17 (2020). <https://doi.org/10.1108/WJE-08-2020-0351>.
- [31] U.L. Ezeamaku, O.D. Onukwuli, M.E. Ezech, I.O. Eze, N.E. Odimegwu, C.P. Agu, Industrial Crops & Products Experimental investigation on influence of selected chemical treatment on banana fibre, Ind. Crop. Prod. 185 (2022) 115135. <https://doi.org/10.1016/j.indcrop.2022.115135>.
- [32] O.D. Onukwuli, E.M. Ezech, R.S. Odera, Effect of different chemical treatment on the properties of banana peduncle fibres, J. Chinese Adv. Mater. Soc. 6 (2018). <https://doi.org/10.1080/22243682.2018.1555056>.
- [33] S.P. Gairola, Y. Tyagi, N. Gupta, MECHANICAL PROPERTIES EVALUATION OF BANANA FIBRE REINFORCED POLYMER COMPOSITES: A REVIEW, Acta Innov. 2022 (2022). <https://doi.org/10.32933/ActaInnovations.42.5>.
- [34] M.J.P. Naik, J. Debbarma, M. Saha, A. Bhargava, Graphene oxide nanoflakes from various agrowastes, Materwiss. Werksttech. 51 (2020). <https://doi.org/10.1002/mawe.201900061>.
- [35] K. Jubair, M.S. Islam, D. Chakraborty, Investigation of Mechanical Properties of Banana-Glass Fiber Reinforced Hybrid Composites, J. Eng. Adv. (2021). <https://doi.org/10.38032/jea.2021.04.002>.